DESIGN AND SYNTHESIS OF NEW ULK1/2 INHIBITOR AS ANTICANCER AGENT

Ph.D. SYNOPSIS

Submitted
to

Gujarat Technological University
Ahmadabad for the award of

DOCTOR OF PHILOSOPHY

In
Pharmacy (Pharmaceutical Chemistry)

By

Sidat Parin Salim
Enrollment No:189999901017

Under supervision of
Dr. M. N. Noolvi M.Pharm., Ph.D.

Shree Dhanvantary Pharmacy College,
Kim, Surat-39 4110, Gujarat.

INDEX

1. TITLE: DESIGN AND SYNTHESIS OF NEW ULK1/2 INHIBITOR AS ANTICANCER AGENT

Abstract

Autophagy initiation kinase 1 and 2 (also known as ULK1/2 in humans) is a protein kinase that plays a key role in the initiation of the autophagy process. Autophagy is a cellular process in which the cell breaks down and recycles its own components, such as damaged or unnecessary proteins and organelles. This process helps the cell to maintain homeostasis and can also play a role in response to stress, such as starvation. In autophagy machinery various genes and enzymes are involved, among that most promising enzyme is ULK1 (Unc-51 like autophagy activating kinase 1). ULK1 is activated by various stress signals, such as nutrient deprivation, and phosphorylates other proteins to initiate the formation of the autophagosome, which is the membrane-bound structure that encloses the material to be degraded during autophagy. ULK1 has been found to play a role in the development and progression of non-small cell lung cancer (NSCLC). Research has shown that ULK1 is involved in promoting tumor cell proliferation, invasion and resistance to chemotherapy and radiation therapy. And ULK2 (Unc-51 like autophagy activating kinase 2) may have additional functions beyond autophagy regulation, such as in cell migration, embryonic development, and neuronal survival. Inhibiting ULK1 has been found to sensitize NSCLC cells to chemotherapy and radiation, suggesting that targeting ULK1 may be a promising strategy for treating NSCLC. In the present research proposal aims at the design of new series of heterocyclic rings like Thiadiazole, quinazoline, benzimidazole, pyrimidine and aniline derivatives as ULK ½ inhibitors. Initial in-silico studies of Ligand based pharmacophore modelling, Molecular docking, Molecular dynamic simulation, DFT and Drug-likeness assessment were done to strengthen the rationale of the study. Based on the literature review different synthetic routes were adopted to synthesize aforementioned heterocyclic compounds. A new series of nitrogen and sulfur containing heterocyclic compounds were synthesized and characterized by using spectral analysis such as IR, ^{1}H NMR and MASS. The synthesized compounds were tested for *In-vitro* 96 well MTT assay on A549 cell line (NSCLC) with Cisplatin as positive control. Compounds **12(b-IV), 12(c-II), 12(b-I), 12(d-IV), 12(f-IV)** and **12(a-II)** showed maximum inhibition IC_{50} value respectively (12.2 µM, 16.35 µM, 20.61

μM, 20.76 μM, 22.01 μM, and 32.04 μM) against Non-small cell lung cancer (A549) cell line, which is more potent or equivalent to cisplatin (33.09 μM) as standard drug.

2. BRIEF DESCRIPTION ON THE STATE OF THE ART OF THE RESEARCH TOPIC.

There is no scarier diagnosis in most people's minds than cancer. Cancer is frequently regarded as an incurable, excruciatingly painful disease with no cure. This perspective of cancer, although prevalent, is overstated and over-generalized. Cancer is unquestionably a serious and potentially fatal disease (1). For example, it is the leading cause of death in those under the age of 85 worldwide, and the second greatest cause of death in people over the age of 85. The truth is that there are many different varieties of cancer, many of which can now be properly treated in order to eliminate, lessen, or slow the effects of disease on people' lives (2). While a cancer diagnosis can still leave patients feeling helpless and out of control, there are many reasons for hope today rather than despondency. Despite advances in diagnosis and treatment, overall patient survival remains low. Until recently, patients' typical treatment options included surgery, chemotherapy, radiation, and endocrine therapy. In this work, we are focussing on Non-small cell lung cancer (NSCLC). Non-small cell lung cancer (NSCLC) is the most common type of lung cancer, accounting for approximately 85% of all lung cancer cases. It includes several subtypes, the most common of which are adenocarcinoma, squamous cell carcinoma, and large cell carcinoma (3). Three types of pathways are mostly involved in cancer cell killing. Apoptosis, necrosis, and autophagy all play significant roles in the cell death process. Aside from that, autophagic cell death is quite useful in nutrient-depleted environments. Some kind of target is required for autophagy induction. ULK1/2 inhibitors are the most useful targets in autophagic processes. At the moment, this target is mostly employed to activate autophagy (4). Under starvation conditions, the mTOR inhibitor is inactive while ULK ("Human autophagy initiation kinase") is active. The primary goal of this research is to design and synthesize some new ULK1/2 inhibitors as anti-cancer medicines. Here, we are proposed Some heterocyclic moieties contains molecules. We are using Thiadiazole, Quinazoline, Benzimidazole and some another aniline derivative for proposing a novel molecule. Before, synthesizing the molecule we used some computational approach for finding stable ligand (5). We finding better ligand by using ***In silico*** study. From that, we are performing Pharmacophore modelling, MD Simulation and Docking. The pharmacophore models can be used to discover potential drug interactions with

drug-metabolizing enzymes by matching the analogous chemical groups of test molecules to those of drug molecules having a well-known ADME-tox profile. Molecular dynamics (MD) is another approach for the investigation of the atom location in space (6). MD is frequently used to simulate the time-dependent motions (trajectories) of biological macromolecules (proteins and RNAs). Forces operating on atoms (particles) in standard MD implementations are calculated as derivatives of potentials. The molecular docking approach can be used to mimic the interaction between a small molecule and a protein at the atomic level, allowing us to characterize small molecule behaviour in target protein binding sites as well as elucidate key biochemical processes (7). All factors are quite useful in determining ligand stability and potency. Draggability indicators such as Lipinski and bioactivity score are also used in this study.

3. DEFINITION OF THE PROBLEM

Since September 2021, non-small cell lung cancer (NSCLC) remained a major area of research and clinical focus in the field of oncology. NSCLC is the most common type of lung cancer, accounting for about 85% of all cases. It encompasses several subtypes, including adenocarcinoma, squamous cell carcinoma, and large cell carcinoma. In the context of NSCLC, researchers have been studying the role of autophagy and exploring whether it could be a potential target for therapy. Some of the strategies and molecules being investigated as potential targets for modulating autophagy in NSCLC include: Inhibitors of Autophagy, Targeting Autophagy-Related Genes and Combination Therapies. Autophagy is a cellular process that involves the degradation and recycling of damaged or unnecessary cellular components, helping to maintain cellular homeostasis and survival. In cancer, including non-small cell lung cancer (NSCLC), the role of autophagy can be complex and context-dependent. Autophagy can both promote tumor growth by providing nutrients to cancer cells under stress conditions and act as a tumor suppressor by eliminating damaged cells (8)(9). The scientific interest in autophagy research lastly culminated in 2016 with the award of **Nobel Prize for Medicine and Physiology to Professor Y. Oshumi** for the discovery, in the early ‘90, of *ATG* genes (autophagy-related genes), controlling and regulating autophagy in yeasts (10)**.**

4. OBJECTIVES AND SCOPE OF WORK

Taking the advantage of thiadiazole, benzothiazole and quinazoline as anticancer agents, the substitutions and molecular hybridization on these heterocyclic compounds would develop a potential class of anticancer agents. A new series of 5-substituted- 1,3,4-thiadiazoles scaffold

with quinazoline and different amine derivatives were proposed. Considering the magnitude of the necessity of ULK1/2 inhibitors, the present research proposal aims at the design and synthesis of ULK1/2 inhibitors as potential anti-cancer agents.

4.1 OBJECTIVES

1. To check the novelty of proposed 5-substituted -1,3,4-thiadiazol-2amine derivatives.
2. To perform *in-silico* studies of different structures including the proposed molecules.
3. To establish the method to synthesize the proposed 5-substituted-1,3,4-thiadiazol-2-amine derivatives.
4. To purify and characterize the proposed molecules by using various methods like TLC, melting point, 1H NMR spectroscopy, 13C NMR spectroscopy, Mass Spectrometry, elemental analysis etc.
5. To evaluate synthesized derivatives on various cancer cell lines at Gujarat University for *in- vitro* anticancer activity.

4.2 SCOPE OF WORK

- New class of ULK1/2 will be developed.
- Publications in international journals of high impact factors.
- Presentation of results in international and national conferences.

5. ORIGINAL CONTRIBUTION BY THE THESIS

To achieve above stated objective the experimental plan of work has been classified in to the following section:

1. Pharmacophore modelling of synthesized compound.
2. Molecular docking analysis of designed compounds.
3. Molecular Dynamics analysis.
4. In silico ADME analysis.
5. Synthesis of molecules.
6. Characterization of synthesized molecules.
7. Biological activity of the synthesized compound.

6. METHODOLOGY OF RESEARCH

6.1 Pharmacophore identification

Pharmacophore modelling is a computational method used to predict the structural features of molecules that are required to bind to a specific target, such as a protein or a receptor.

The main idea behind pharmacophore modelling is to identify the common features of known ligands (molecules that bind to a specific target) and use that information to predict the properties of new ligands (11,12).

6.2 Molecular Docking

Docking helps to decide if a candidate drug will interact appropriately with a target receptor protein. Molecular docking is one of the most frequently used methods in structure-based drug design, due to its ability to predict the binding-conformation of small molecule ligands to the appropriate target binding site (13,14).

6.3 Molecular dynamics

Molecular dynamics (MD) simulation is a computational technique that uses classical mechanics to study the motions of atoms and molecules over time. In MD simulations, the behaviour of a system is modelled as a collection of particles, and the forces acting on each particle are calculated using physical laws, such as Newton's laws of motion (15,16).

6.4 Drug-likeness and in-silico ADMET prediction

The drug-likeness and pharmacokinetic properties of the designed compounds were evaluated using SwissADME and pkCSM. Drug-likeness of compounds was predicted based on various rules like Drug likeness refers to the degree to which a molecule possesses properties that are associated with successful drugs (17,18).

7. EXPERIMENTAL METHOD

7.1 Materials and Methods

7.1.1 Reaction Scheme (19,20)

Scheme-1:

Synthesis of 5-Substituted Phenyl -1,3,4-thiadiazole-2-amine **3a-3h** by using Different aromatic carboxylic acids with thiosemicarbazide (2) in presence of Phosphorus oxychloirde as dehydrating agent and final cyclization using water.

Scheme-2:

Urea (460 mmol) was heated to melt, then 2-methylaminobenzoic acid (46 mmol) was added. The mixture was stirred for 5 h at 150˚C and then cooled to below 100˚C. Water (70 mL) was added to quench the reaction. The precipitated was collected and recrystallized in a mixed solution of acetone (10 mL) and water (100 mL) to afford compound **6** as a white powder.

Scheme-3:

2,4-dichloroquinazoline was obtained by refluxing 10.0g (0.061 mole) of quinazoline-2,4(1H,3H)-dione(Benzoylene urea) in 14.2g(0.092 mole) of Phosphorous oxychloride with 7.4g(0.061mole)N,N-dimethylaniline at 108°C . The progress of the reaction was monitored by TLC (Eluent: ethyl acetate: hexane=7:3). After the completion, the reaction mass was cooled to room temperature and hence poured onto ice water under stirring. An off-white viscous precipitate formed. The resultant mass was basified with Aqueous 20% w/v of Potassium carbonate to ph 8.0. After reaching the mentioned pH, the reaction mass was extracted with 200.0 ml Dichloromethane. The dichloromethane layer was given a water wash, dried over sodium sulphate and hence distilled to obtain 5.0 g 2, 4- dichloroquinazoline **7**.

Scheme-4:

DIPEA (0.951ml, 5.3 mmol) was added to a suspension of 2,4 dichloo quinazoline (370 mg, 1.85 mmol) and 5-Phenyl-1,3,4-thiadiazol-2-amino (250mg,0.75mmol) in ethanol (10 ml). The Suspension was stirred at 25 C for 24 hrs. The resulting precipitated was filtered and washed with ethanol to afford **10a-10h** as a white solid.

Scheme-5:

A mixture of **10a-10h** (24.3mg, 0.081mmol), and aniline derivatives (55.4mg, 0.416mmol) in ethanol (1.5 ml) was stirred at 120˚ C in a sealed vial for 1.5 h. and the reaction mixture was cooled and purified with suitable solvent, obtained **12I-12-V.**

7.2 EXPERIMENTAL METHOD

Step-1: Synthesis of Substituted 5-phenyl-1,3,4-thiadiazole-2-amine.

(Cyclization reaction)

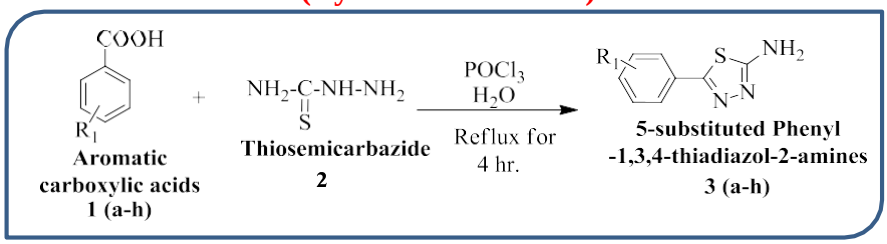

Step-2: Synthesis of Quinazoline-2, 4 (1H, 3H)-dione.

(Condensation and Cyclization reaction)

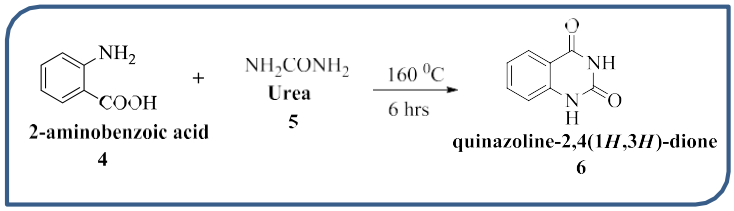

POSSIBLE DERIVATIVES OF SCHEME 1 and 2

COMPOUND	R	COMPOUND	R
3-a, 6-a	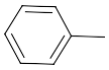	3-e, 6-e	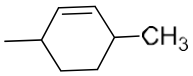
3-b, 6-b	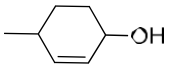	3-f, 6-f	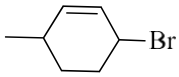
3-c, 6-c	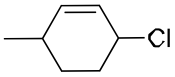	3-g, 6-f	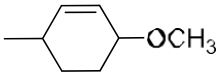
3-d, 6-d	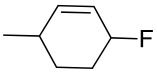	3-h, 6-h	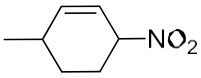

Step-3: Synthesis of 2,4-dichloroquinazoline. (Chlorination reaction)

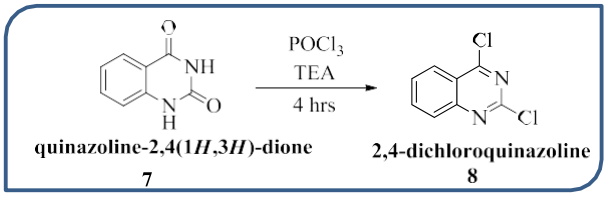

Step-4: Synthesis of N-(2-chloroquinazolin-4-yl)-5-phenyl-1,3,4-thiadiazol-2-amine. (Substitution reaction)

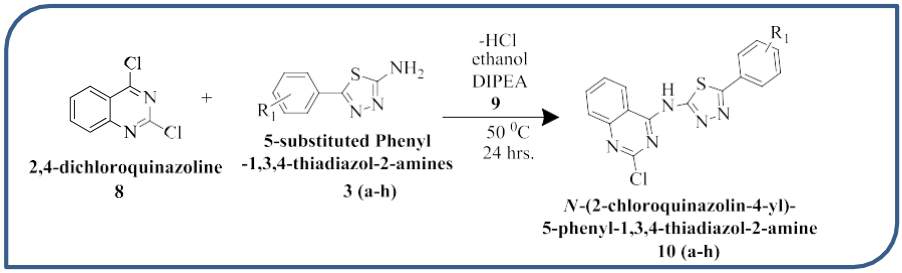

Step-5: Synthesis of N2-(6-methylpyridin-2-yl)-N4-(5-(p-tolyl)-1,3,4-thiadiazol-2-yl) -4a, 8a-dihydroquinazoline-2,4-diamine (Substitution reaction)

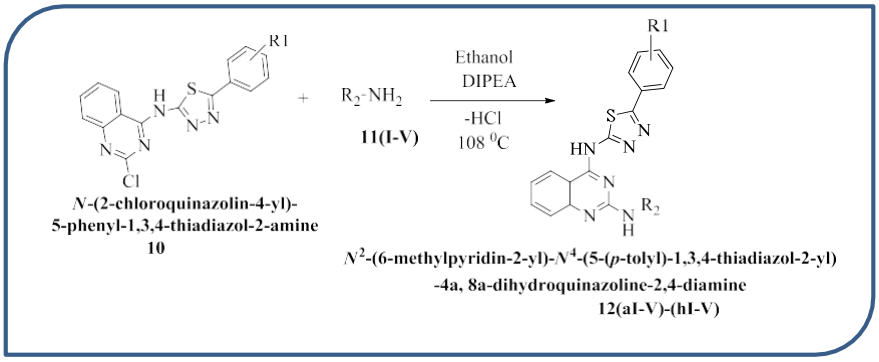

PREPARED DERIVATIVES

COMP.	R_1	R_2	COMP.	R_1	R_2
12 (a-I)	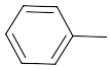	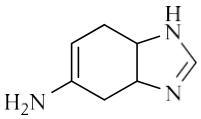	**12 (c-II)**	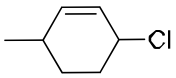	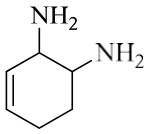
12 (a-II)	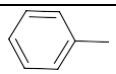	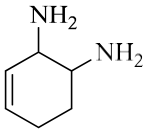	**12 (c-IV)**	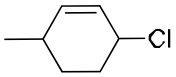	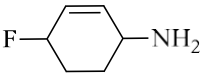
12 (a-III)	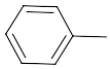	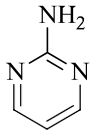	**12 (d-II)**	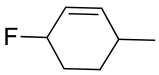	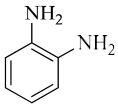
12 (a-IV)	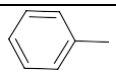	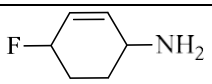	**12 (d-IV)**	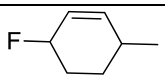	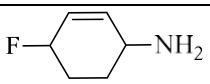
12 (a-V)	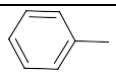	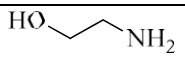	**12 (e-IV)**	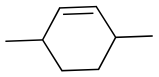	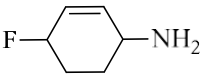
12 (b-I)	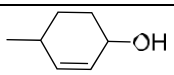	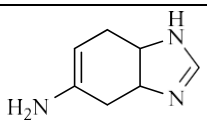	**12 (e-V)**	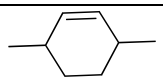	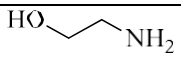
12 (b-III)	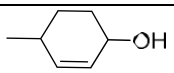	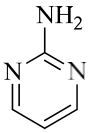	**12 (f-IV)**	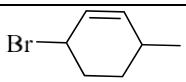	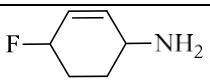
12 (b-IV)	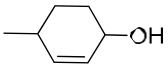	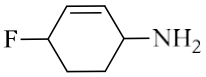	**12 (f-V)**	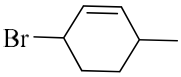	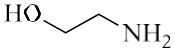

7.3 Biological activity of the synthesized compound

7.3.1 Cell Lines and Culture

The A549 cell line, derived from human lung cancer and has a wild-type p53 gene, was obtained from the National Centre for Cell Science (NCCS) in Pune, Maharashtra, India. The cells were cultured in F-12K, Eagle's Minimum Essential Medium (EMEM), and RPMI1640 mediums at 37 °C in 5% CO_2. The cell lines were regularly checked for Mycoplasma and Epstein-Barr Virus presence to ensure their purity.

7.3.2 In vitro antiproliferative assay (MTT Assay)

The antiproliferative effects of the synthesized compound were assessed using the MTT (3-(4,5-dimethylthiazol-2-yl)-2,5-diphenyltetrazolium bromide) assay. The A549 cell line was seeded at a density of 104 cells per well in 96-well plates and allowed to adhere for 24 hours at 37°C with 5% CO_2. Triplicate wells with varying concentrations of the test compounds (0.01, 0.1, 1, 10, 100, and 1000 µM) were then treated for 24 hours, with cisplatin serving as a positive control and untreated cells as blanks. After incubation, MTT solution (5 mg/mL) was added to each well and incubated further for 4 hours in the dark at 37°C. The resulting purple-colored formazan crystals were dissolved in DMSO, and the optical density (OD) was recorded at 570 nm using a microplate spectrophotometer. Blanks containing media without cells were included. The IC50, the concentration at which 50% of cell growth was inhibited, was calculated using GraphPad software by comparing the OD reading with the control.

7.4 Result and Discussion

In-silico techniques increase the effectiveness of the drug discovery process and reduce the experimental cost and time. The selected protein structure was subjected to stereochemical and quality evaluation using PROCHECK and ProSA-web servers, while the binding site analysis was performed using CASTp servers. Ramachandran plot revealed that 92.6% residues are present in favoured regions, as shown in (**Figure 4a)**. The z-score indicating overall model quality for prepared protein structure was found to be -6.4. (Figure 3b) represents a plot showing the z-scores of all experimentally determined protein chains in PDB: 4WNP. A single pocket was detected in the targeted protein (PDB: 4WNP) with an area of 6341.321 and a volume of 15204.689 (**Figure 5**).

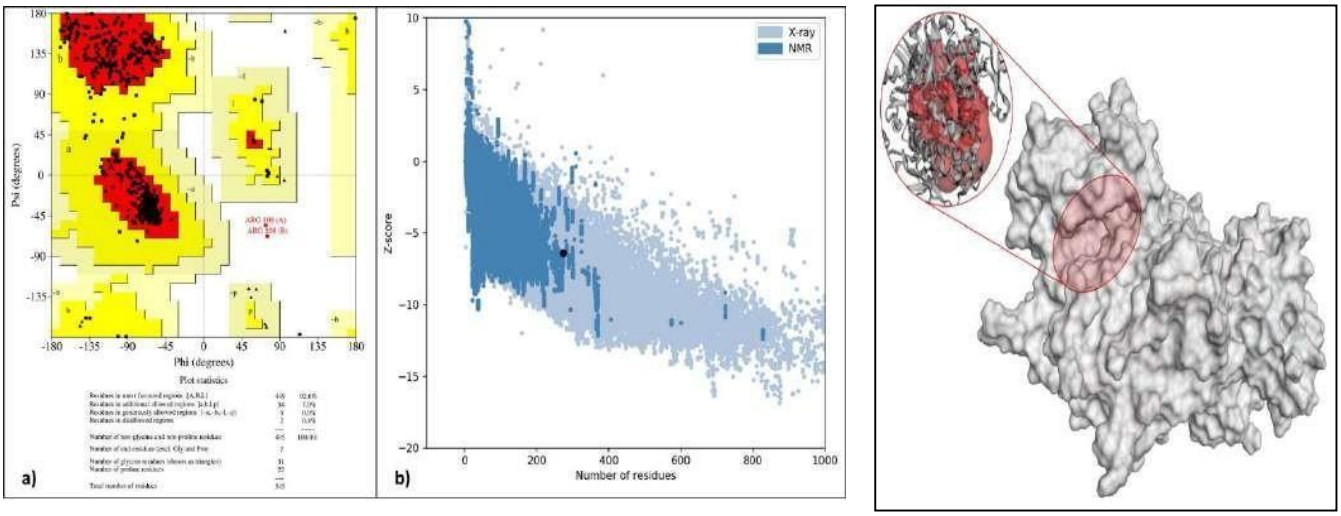

Figure 4. a) Ramachandran plot of the target protein (PDB: 4WNP) showing 86.6% residues in the favoured region, **b)** Plot showing the z-scores. and **Figure 5**. Binding pocket (red) of 4WNP observed from CASTp server.

7.4.1 Molecular docking

A molecular docking study was performed to determine the binding energies and best binding confirmations using designed compounds with ULK1 (PDB: 4WNP). AutoDock Vina package of PyRx 0.8 software was used to carry out the molecular docking study. Ligand library of 46 compounds containing designed compounds, five standard molecules from literature and naturally attached ligand in protein structure were docked against ULK1 (PDB: 4WNP). 3RJ (PubChem CID: 86346643) is a naturally attached ligand in protein structure that was used as one of the standards to compare the docking results of designed compounds.

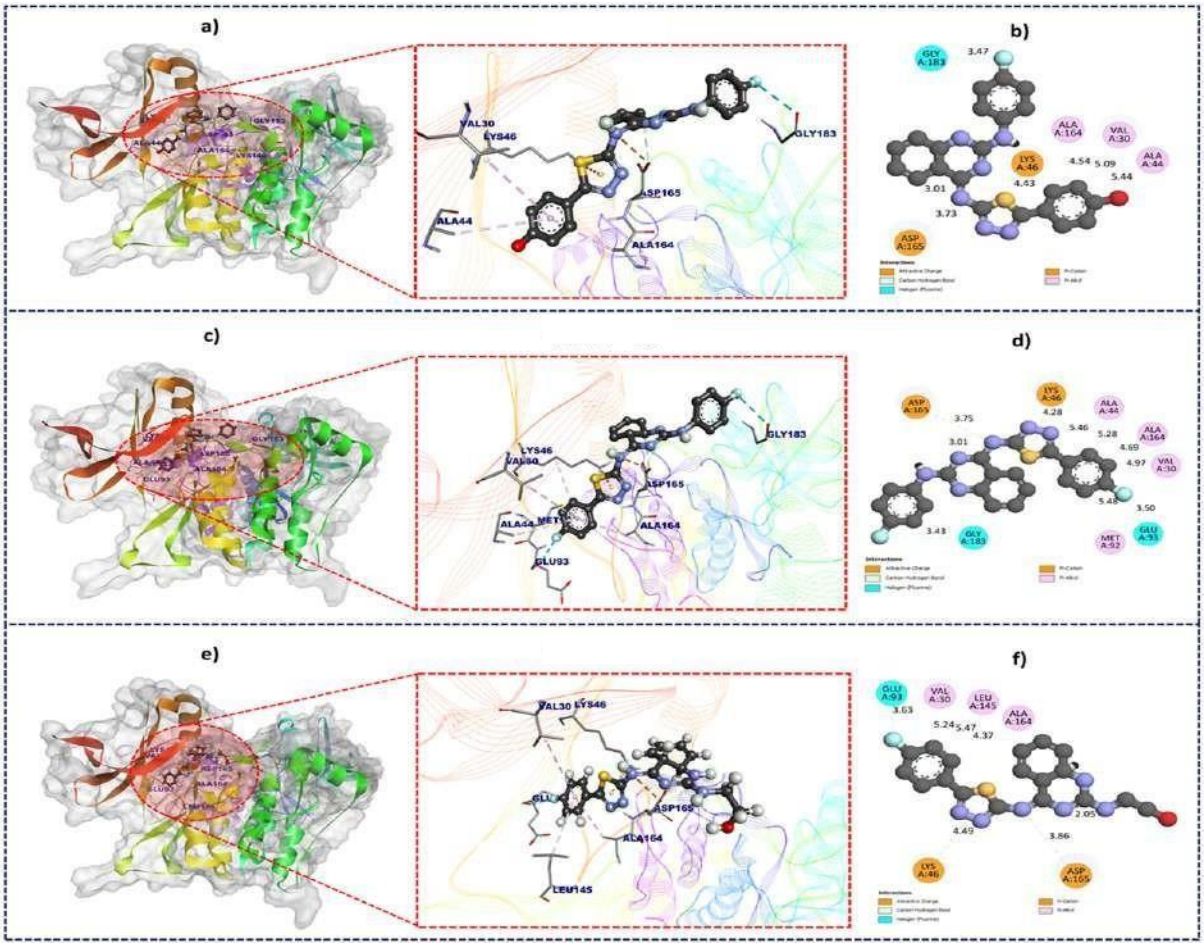

Figure 6. 2D and 3D interactions of protein-ligand complexes having good binding affinity. a) 12(b-IV) ligand (-11.3 kcal/mol), b) 12 (c-II) ligand (-11.0 kcal/mol), and c) 12 (b-I) (11.2 kcal/mol).

Table 2 represents the hydrophobic interactions, hydrogen bonds, and distance between designed compounds and ULK1. The BIOVIA Discovery Studio Visualizer was used to determine detailed 2D and 3D interactions. **Figure 6** depicts 2D and 3D visualizations of interactions between top-ranked protein-ligand complexes.

Table 2: Binding energy, hydrophobic interactions, hydrogen and hydrogen bond distance of a ULK and the designed compounds.

Compound ID	Binding Energy (kcal/mol)	Hydrophobic Interactions	Hydrogen Bonds	Hydrogen Bond Distance (Å)
12a-I	-10.3	ASP102, GLY23, LYS140, ILE22, ASP143, ALA164, VAL176, MET92.	LYS46, HIS24	2.99 and 3.30
12a-II	-10.2	LEU145, VAL176, ASP99, GLY23, HIS24, LYS46, ASP146, PHE168	-	-
12a-III	-10.4	LEU59, ALA28, PHE27, GLY167 LYS46, GLN142, LYS46, ASN143, ASP165, CYS95, VAL130, GLU93 LYS46, LEW145	LYS64	3.12
12a-IV	-10.9	PHE168, ALA28, LEW59, LYS46, GLU143, LYS46, ASP165, GLU165, GLN142, LEU145, VAL130.	-	-
12a-V	-9.5	ALA28, PHE168, ASP165, LEU59, GLU160 LYS46, LEU60, MET92, VAL130, ALA44	-	-
12b-I	-10	LEU59, ALA28, PHE27, GLY167 LYS46, GLN142, ASN143, ASP165, LEU145	CYS95	2.88
12b-II	-10.4	TYR79, ARG255, LEU246, ALA249, PHE70, GLY151, LEU246, GLU73, GLN142, LYS162, ASN143, ASP165,	SER147, GLU271	2.83, 3.29, 3.13 and 3.18
12b-III	-9.8	GLU73, TYR79, LEU256, LYS256, TYR94, LEW41, ARG160, GLN253, GLY42, ASN96, PRO149	-	-
12b-IV	-11.3	GLY167, PHE27, LEU59, ALA28, LEU60, ASP165, GLY25, ASN143, LYS46, LEU145, LEU145, VAL76, PHE168	-	-
12b-V	-9.6	GLN253, ARG160, TYR94, SER147, GLU73, ASN148, PRO149, GLU42,	LYS162, ASN96	3.02 and 3.03

		GLY271		
12c-I	-9.1	VAL176, LEU145, GLY98, TYR94, ILE22, VAL130, MET92, ASP165, HIS24, ALA28, LYS46	ASN143	3.17
12c-II	-10.7	LEW59, PHE169, ALA26, LEU60, LYS146, VAL130, ILE22	-	-
12c-III	-9.2	PHE168, GLY25, LYS46, LEW59, ALA28, GLY167, VAL130, ILE22, ALA44	-	-
12c-IV	-10.8	LYS140, GLY183, ASP138, PHE168, LEW59, ALA28, ASP165, LEW60, VAL130, ILE22	-	-
12c-V	-10	LEU59, PHE168, ALA28, ASP165, VAL130, LEW145, ALA164	LYS140, LYS146	2.98 and 3.01
12d-I	-10.5	ILE22, VAL130, LEU145, ASP120, HIS24, LYS146, GLY25, ALA28, ASP165, GLN142	ASP99	3.28
12d-II	-9.7	PHE168, ALA28, HIS24, ASP165, LEU145, GLN142, GLY25,	ASN143	3.22
12d-III	-10	PHE168, LEU59, ASP165, HIS24, ALA164, GLU93, LEU145, VAL167,	LYS64, ASN143	3.23 and 2.98
12d-IV	-11	SER184, ASP138, GLY25, ASN143, LYS46, LEU145, ALA44, ALA164, VAL76, VAL30, GLU93, MET92, PHE168, CYS182	-	-
12d-V	-11.2	LYS140, SER184, PHE168, PHE27, ALA28, LEU59, GLY167, ASP165, MET92, ALA44, VAL76, GLU93,	-	-
12e-I	-10.6	GLN142, PHE168, ALA28, PHE27, ASP165, ALA164, LEU59, VAL130, GLU93	LYS46	2.98
12e-II	-10.6	LYS140, PHE27, LEU59, VAL130. ALA164, VAL176, ASP165, LEU145, GLU93	-	-
12e-III	-10.7	GLY25, ASP165, LYS14, GLU142, VAL130, LEU145, ILE22, ALA44, CYS95, VAL130	-	-
12e-IV	-9.7	PHE168, ASP165, LEU59, ALA28, VAL130, ALA164, LEU145, ASP146	LYS140, LYS46	3.20 and 3.25
12e-V	-8.3	PHE27, ALA126, ASP165, LYS140, VAL130, GLY98, ASP99, ILE22.	ASN143, GLN142,	3.18, 3.29

		CYS95	TYR94	and 2.78
12f-I	-9.5	PHE168, ASP165, ALA28, GLY25, GLU142, VAL130, LYS46, ALA44, MET92	-	-
12f-II	-9.2	LEU60, GLY167, LYS46, HIS24, ALA28, ASP165, VAL130, ALA44, TYR94	-	-
12f-III	-9.3	PHE27, LY46, ALA28, GLY25, HIS24, LEU59, ALA44, VAL130	-	-
12f-IV	8.3	LEU59, ALA28, LEU60, ASP165, GLY25, HIS24, LYS46, ILE22	GLU163	2.91
12f-V	-10.3	LYS46, VAL130, GS24, PHE27, GLY183, PHE168, ASP165, LY25, LEU60, HIS24, CYS182	-	-
12g-I	-10.7	ASP138, GLU59, ALA28, VAL13 LYS140, PHE168, ASP165	SER184	3.24
12g-II	-9.6	LEU59, PHE168, LYS46, GLN142, VAL130, ALA28	-	-
12g-III	-10.4	LYS162, ALA28, LEU41, GLN253, ASP40, GLY151, ARG152, PRO276	SER147, GLU142	3.32 and 3.04
12g-IV	-9.7	PHE27, ALA28, ASP146, LEU59, VAL130, ALA164	LYS140, LYS46	2.97 and 3.10
12g-V	-8.9	ALA26, GLN142, PHE27, HIS24, ASN143, GLY25, ASP146, VAL130, LEU145, LYS46	-	-
12h-I	-9.0	LYS46, ALA44, VAL176, GLN93, GLY25, CYS95, ILE22, GLY9	TYR94	2.81
12h-II	-8.9	LEU172, ASP199, PHE268, SER174, HIS130, GLY133, HIS274	ARG127, ASP270	3.25 and 3.06
12h-III	-9.2	ALA26, GLY25, HIS24, PHE168, ASN143, LEU59, LYS46, ALA44, ASP165, MET92, VAL130	-	-
12h-IV	-8.3	ALA28, PHE168, GLN142, LYS140, GLY23, ILE22, ALA44, ASP165, TYR94	ASN143, CYS95	3.17 and 3.16
12h-V	-8.0	GLY25, HIS24, PHE168, ASN143, LEU59, LYS46, ALA44, ASP165, MET92, VAL130		
STD1	-9.3	ALA26, GLY25, HIS24, PHE168, ASN143, LEU59, LYS46, ALA44,	GLU95,	2.91 and

		ASP165, MET92, VAL130	CYS92	2.92
STD2	-8.9	LEU172, ASP199, PHE268, SER174, HIS130, GLY133, HIS274	-	-
STD3	-9.0	PHE168, ASP165, ALA28, GLY25, GLU142, VAL130, LYS46, ALA44, MET92	-	-
STD4	-9.0	LEU172, ASP199, PHE268, SER174, HIS130, GLY133, HIS274	-	-
STD5	-9.0	ASP165, ALA28, GLY25, GLU142, VAL130, LYS46, ALA44, MET92	-	-
3RJ (PubChem CID: 86346643)	-10.7	PHE273, ILE135, HIS130, PHE269, LEU129, SER131, ILE134, HIS130, GLY133, GLY200, LEU172, ASP199, SER174, GLY,133 GLN173, LEU172,	SER131	2.33

7.4.2 Pharmacophore analysis

Pharmacophore modelling was done using PharmaGist server to generate the scored sets of pharmacophoric features. All designed compounds aligned together with the pivot molecule. The best pharmacophore model was selected based on pharmacophoric features showing high score, and to the multiple alignments of designed compounds. The quantitative characteristics of the best-scored pharmacophore model are shown in **Table 3.** The highest ranked pharmacophore model with a score of 97.500 was selected for spatial feature analysis. Geometric characterization of the highest scored pharmacophore model is represented in (**Figure 6)**.

Table 3. Generated pharmacophore models from PharmaGist Tool.

Pharmacophore model	Score of the pharmacophore model	Spatial features	Aromatic ring	Hydrophobic	Hydrogen donor	Hydrogen acceptor
1	97.500	10	3	0	3	4
2	97	11	3	1	3	4
3	90	9	3	0	2	4
4	82.500	9	2	0	3	4
5	82.500	8	3	0	2	3
6	80.777	7	3	0	1	3
7	75	8	2	0	3	3

8	75	8	2	0	2	4
9	75	8	2	0	2	4
10	74.954	9	2	1	3	3

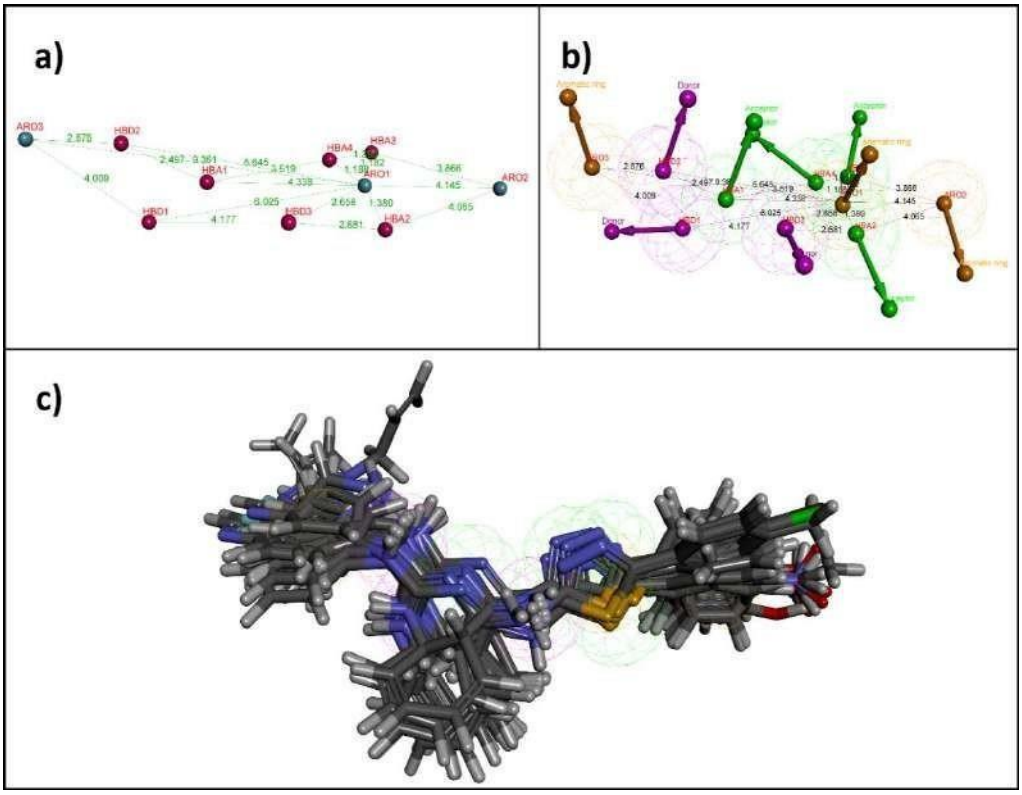

Figure 6. Characteristics of the best pharmacophore model having best score. (a) Geometric distance. (b) Pharmacophoric features. (c) Aligned molecules

7.4.3 Drug-likeness and *in-silico* ADMET prediction

Drug-likeness and *in-silico* ADMET studies were performed to determine the drug-like candidates from designed compounds. Prediction of drug-likeness of designed compounds was done based on Lipinski's rule of five, Veber's rule, Ghose's rule, Egan's rule, and Muegge's rule, which are commonly used methods to determine the drug-like properties of compounds. All the designed compounds followed Lipinski's rule of five with minimum or zero violation in rule except 8a does not follow Lipinski's criteria. Therefore, designed compounds are present within an acceptable range of drug-likeness properties with minimum violations in Lipinski's rule of five as shown in **Table 5**.

Table 5. Lipinski's rule of five and Drug-likeness prediction of designed compounds.

Compound	Lipinski's rule of five					Lipinski's violations	Drug likeness				
	MW	mLogP	nHBA	nHBD	MR		Lipinski	Veber	Ghose	Egan	Muegge
12a-I	478.57	3.41	5	2	149.67	0	Yes	Yes	No	Yes	Yes
12a-II	413.5	3.16	4	3	130.38	0	Yes	Yes	No	Yes	Yes
12a-III	400.46	2.07	6	2	121.56	0	Yes	Yes	Yes	Yes	Yes
12a-IV	416.47	4.07	5	2	125.93	0	Yes	Yes	Yes	Yes	Yes
12a-V	366.44	1.94	5	3	110.72	0	Yes	Yes	Yes	Yes	Yes
12b-I	494.57	2.9	6	3	151.69	0	Yes	No	No	No	Yes
12b-II	429.5	2.64	5	4	132.4	0	Yes	No	No	No	Yes
12b-III	416.46	1.97	7	3	123.59	0	Yes	No	Yes	No	Yes
12b-IV	432.47	3.54	6	3	127.95	0	Yes	Yes	Yes	Yes	Yes
12b-V	382.44	1.83	6	4	112.75	0	Yes	No	Yes	No	Yes
12c-I	513.02	3.88	5	2	154.68	1	Yes	Yes	No	Yes	Yes
12c-II	447.94	3.65	4	3	135.39	0	Yes	Yes	No	Yes	Yes
12c-III	434.9	2.97	6	2	126.57	0	Yes	Yes	Yes	Yes	Yes
12c-IV	450.92	4.55	5	2	130.94	1	Yes	Yes	No	Yes	Yes
12c-V	400.89	2.85	5	3	115.73	0	Yes	Yes	Yes	Yes	Yes
12d-I	496.56	3.78	6	2	149.62	0	Yes	Yes	No	Yes	Yes
12d-II	431.49	3.54	5	3	130.33	0	Yes	Yes	No	Yes	Yes
12d-III	418.45	2.86	7	2	121.52	0	Yes	Yes	Yes	Yes	Yes
12d-IV	434.46	4.45	6	2	125.89	1	Yes	Yes	Yes	Yes	Yes
12d-V	384.43	2.73	6	3	110.68	0	Yes	Yes	Yes	Yes	Yes
12e-I	478.57	3.41	5	2	149.67	0	Yes	Yes	No	Yes	Yes
12e-II	427.52	3.38	4	3	135.34	0	Yes	Yes	No	Yes	Yes
12e-III	414.49	2.7	6	2	126.53	0	Yes	Yes	Yes	Yes	Yes
12e-IV	430.5	4.28	5	2	130.9	1	Yes	Yes	No	Yes	Yes
12e-V	380.47	2.58	5	3	115.69	0	Yes	Yes	Yes	Yes	Yes
12f-I	508.6	3.11	6	2	156.16	1	Yes	Yes	No	Yes	Yes
12f-II	427.52	3.38	4	3	135.34	0	Yes	Yes	No	Yes	Yes
12f-III	430.49	2.19	7	2	128.05	0	Yes	Yes	Yes	No	Yes
12f-IV	446.5	3.75	6	2	132.42	0	Yes	Yes	No	Yes	Yes
12f-V	396.47	2.06	6	3	117.22	0	Yes	Yes	Yes	No	Yes
12g-I	557.47	3.98	5	2	157.37	1	Yes	Yes	No	Yes	Yes
12g-II	492.39	3.75	4	3	138.08	0	Yes	Yes	No	Yes	Yes

12g-III	479.36	3.08	6	2	129.26	0	Yes	Yes	Yes	Yes	Yes
12g-IV	495.37	4.66	5	2	133.63	1	Yes	Yes	No	Yes	Yes
12g-V	445.34	2.96	5	3	118.42	0	Yes	Yes	Yes	Yes	Yes
12h-I	523.57	4.08	7	2	158.49	2	No	No	No	No	No
12h-II	458.5	3.53	6	3	139.2	0	Yes	No	No	No	No
12h-III	445.46	2.47	8	2	130.38	1	Yes	No	No	No	No
12h-IV	461.47	4.41	7	2	134.75	1	Yes	No	No	No	Yes
12h-V	411.44	2.31	7	3	119.55	0	Yes	No	Yes	No	No

Pharmacokinetics of designed compounds (Absorption, Distribution, Metabolism, Excretion, and Toxicity) was characterized virtually with the help of pkCSM servers to determine the ADMET profile of designed compounds. The results of ADMET prediction showed that designed compounds showed good ADME properties, as shown in **Table 6**. Some of them showed positive results in AMES toxicity, and hence they may be mutagenic. *In silico* ADMET profile of the designed compounds was observed with satisfactory results.

7.4.4 Molecular dynamic simulation

As per the molecular docking results, **12b-IV, 12d-IV,** and **12d-V** were identified as hit molecules, showing good binding affinity with the targeted protein structure. The protein-ligand complex systems of targeted protein (PDB: 4WNP) and **12d-IV** were further subjected to molecular dynamic (MD) simulation studies to investigate the conformational stability of the complex. MD simulation was performed using WebGro to determine the time-dependent motions, behavior, and configurational changes between subjected protein-ligand complexes over 100 ns. CABS-flex ver. 2.0 was used to determine the root mean square fluctuation (RMSF) of complex systems. Analysis of MD trajectories was done using parameters such as root mean square deviation (RMSD), root mean square fluctuation (RMSF), the radius of gyration (*R*g), hydrogen bonds (HBs), and principal component analysis (PCA).

The RMSD values were calculated for all frames present in the MD simulation trajectory of each simulated protein-ligand complex. The average change of atom displacement for the 4WNP-4d complex system over 100 ns MD simulation was estimated using RMSD and the structural stability of the complex system was also investigated. These RMSD profiles of the 4WNP-4d complex help to determine the behaviour of the backbone and heavy atoms of the protein. The lower deviations in RMSD values represent the more stable nature of protein and

Protein-ligand complex. Hence, the stability of subjected 4WNP-4d complex was analyzed with the help of RMSD values. And the calculations were done to obtain the equilibrium time of the simulated complexes. Through the results of the RMSD analysis, it is observed that the simulated complex has minimum deviations in the RMSD. **Figure 7a** represents the RMSD plot for the **4WNP-12d-IV** complex. The RMSD values for **4WNP-12d-IV** ranged between 0.4 nm to 0.6 nm, respectively According to the RMSD plot for **4WNP-12d-IV** the complex was stable over 100 ns with a minimum deviation.

The RMSF profile was determined for the protein and protein-ligand complexes (**Figure 7b**). It measures the movement of each residue around the average position along the trajectory, revealing the flexibility of a specific protein region during the MD simulation. **Figure 7b** represents the RMSF of the **4WNP-12d-IV** complex. It was observed that ALA37 (RMSF value: 0.29 nm), ALA36 (RMSF value: 0.4 nm), HIS39 (RMSF value: 0.38 nm), ASP40 (RMSF value: 0.24 nm), ALA150 (RMSF value: 0.29 nm), GLU151 (RMSF value: 0.26 nm), ARG152 (RMSF value: 0.24 nm), ARG153 (RMSF value: 0.25 nm), ALA154 (RMSF value: 0.27 nm), SER174 (RMSF value: 0.31 nm), ASN175 (RMSF value: 0.47 nm), MET176 (RMSF value: 0.33 nm), ALA179 (RMSF value: 0.41 nm) amino acid residues of **4WNP-12d-IV** showed fluctuations in which ASN175, ALA36, ALA179 displayed high fluctuations. However, the RMSF values are lower than the observed RMSD values and remained in the acceptable region, confirming the stability of particular amino acid residues.

*R*g trajectory of MD simulation was computed to assess the overall stability of protein structure during MD simulation. It was also used to determine the compactness of protein due to the presence or absence of ligands over 100 ns. *R*g values for **4WNP-12d-IV** were studied over 100 ns at 300 K. In terms of MD trajectory analysis, the *R*g values for the **4WNP-12d-IV** ranged between 2.6 to 2.7 nm indicating no significant changes after 10 ns. It indicates that protein in presence of 4d, did not show any conformational changes. According to the results of computed *R*g, the simulated complex showed conformational stability with minimum fluctuation in the *R*g values **(Figure 7c)**. Hydrogen bonds (HBs) play a significant role in stabilizing the protein-ligand complex. In addition, HBs responsible for drug specificity, metabolization, and adsorption in the body. HBs maintain the overall confirmation of the simulated complex. Therefore, MD trajectories were also analyzed to examine the time evaluation of the number of HBs between protein-ligand complexes formed during the 100 ns simulation. The number of HBs present in

the 4WNP-4d, complex system with consistent over the 100 ns MD simulation at 300 K **(Figure 7d)**. No significant changes were observed in the hydrogen bond interactions between the **4WNP-12d-IV** complex and a maximum of six hydrogen bonds were observed in the initial phase of MD simulation.

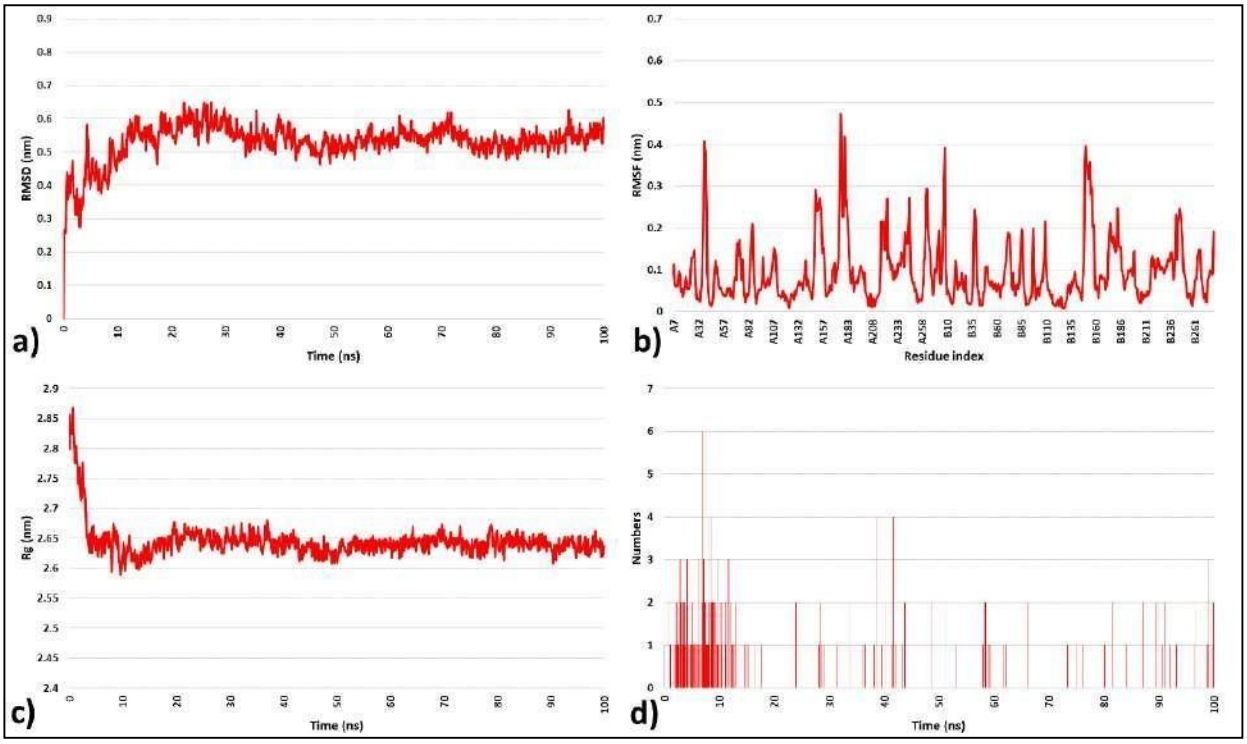

Fig.7. MD Simulation trajectory (A) RMSD (B) RMSF (C) RG (D) H Bond Number

7.5 Characterization of Synthesized Molecules

Step 1:

Sr. No.	Compound Code	R	Mol. Formula	Melting Point °C	R_f Value	FT-IR (KBR, cm^{-1})
1	3a	H	$C_8H_7N_3S$	216-219 °C	0.6	3281 (1° NH), 3088 (C-H), 1518 (C=N), 690(C-S-C)
2	3b	OH	$C_8H_7N_3OS$	218-225 °C	0.8	3398 (OH), 3245 (1° NH), 3011 (C-H), 1503 (C=N), 663 (C-S-C)
3	3c	Cl	C_8H6ClN_3S	216-220 °C	0.6	3037 (1° NH), 2806 (C-H), 1699 (C=N), 765 (C-Cl), 700 (C-S-C)
4	3d	F	$C_8H_7FN_3S$	216-221 °C	0.7	3017 (1° NH), 2956 (C-H), 1669 (C=N), 1163 (C-F-C), 647 (C-S-C)
5	3e	CH_3	$C_9H_9N_3S$	216-220 °C	0.7	3309 (1° NH), 3122 (C-H), 1515 (C=N), 1463 (C-F-C), 654 (C-S-C)
6	3f	Br	$C_8H_7BrN_3S$	216-220 °C	0.8	3274 (1° NH), 3087 (C-H), 1515 (C=N), 759 (C- Br), 690

						(C-S-C)

Step 2 and 3:

Sr. No.	Compound Code	Mol. Formula	Melting Point °C	R_f Value	FT-IR (KBR, cm^{-1})
1	4	$C_8H_6N_2O_2$	277-282 °C	0.8	3508 (2° NH), 3113 (C-H), 1676, 1612 (C=O)
2	6	$C_8H_4Cl_2N_2$	118-120 °C	0.7	3142 (C-H), 1558, 15123 (C=N), 831,752 (C-Cl)

Step 4:

Sr. No.	Compound Code	R	Mol. Formula	Melting Point °C	R_f Value	Spectral Data
1	6a	H	$C_{16}H_{12}ClN_5S$	210-215 °C	0.7	**FT-IR (KBR, cm^{-1})** 3378 (2° NH), 2955 (C-H), 1518 (C=N), 845 (C-Cl), 690(C-S-C) **MASS (m/z %)** 341(M+), 343 (M+2)
2	6b	OH	$C_{16}H_{10}ClN_5OS$	213-216 °C	0.8	**FT-IR (KBR, cm^{-1})** 3649 (OH), 3280 (2° NH), 3091 (C-H), 1518 (C=N), 760 (C-Cl), 690(C-S-C) **MASS (m/z %)** 355 (M+), 357 (M+2)
3	6c	Cl	$C_{17}H_9ClN_5S$	216-219 °C	0.6	**FT-IR (KBR, cm^{-1})** 3387 (2° NH), 2924 (C-H), 1504 (C=N), 833 (C-Cl), 630 (C-S-C) **MASS (m/z %)** 374 (M+), 376 (M+2)
4	6d	F	$C_{16}H_9ClFN_5S$	216-220 °C	0.7	**FT-IR (KBR, cm^{-1})** 3029 (2° NH), 2937 (C-H), 1556 (C=N), 841 (C-Cl), 622 (C-S-C) **MASS (m/z %)** 357 (M+), 359 (M+2)
5	6e	CH_3	$C_{17}H_{12}ClN_5S$	218-222 °C	0.7	**FT-IR (KBR, cm^{-1})** 3281 (2° NH), 3066 (C-H), 1636 (C=N), 841 (C-Cl), 622 (C-S-C) **MASS (m/z %)** 352 (M+), 354 (M+2)
6	6f	Br	$C_{16}H_9ClBrN_5S$	218-223 °C	0.8	**FT-IR (KBR, cm^{-1})** 3319 (2° NH), 3072 (C-H), 1691 (C=N), 769 (C-Cl), 649 (C-S-C)

						MASS (m/z %) 416 (M+)

Step 5:

Sr. No.	Compound Code	Mol. Formula	Melting Point °C	R_f Value
1	12a-I	$C_{26}H_{22}N_8S$	245-250 °C	0.6
2	12a-II	$C_{22}H_{17}N_7S$	246-251 °C	0.7
3	12a-III	$C_{20}H_{14}N_8S$	247-250 °C	0.8
4	12a-IV	$C_{22}H_{17}FN_6S$	248-255 °C	0.6
5	12a-V	$C_{18}H_{18}N_6OS$	248-256 °C	0.8
6	12b-I	$C_{26}H_{22}N_8OS$	250-255°C	0.6
7	12b-III	$C_{20}H_{16}N_8OS$	251-255 °C	0.7
8	12b-IV	$C_{22}H_{15}FN_6OS$	252-258 °C	0.6
9	12c-II	$C_{22}H_{16}ClN_7S$	253-260 °C	0.7
10	12c-IV	$C_{22}H_{14}ClN_6OS$	255-261 °C	0.6
11	12d-II	$C_{22}H_{18}FN_7S$	256-265 °C	0.6
12	12d-IV	$C_{22}H_{14}F_2N_6S$	258-265 °C	0.7
13	12g-IV	$C_{22}H_{14}BrFN_6S$	259-267 °C	0.6
14	12g-V	$C_{18}H_{17}BrN_6OS$	260-267 °C	0.6
s15	12e-IV	$C_{23}H_{17}FN_6S$	260-265 °C	0.7
16	12e-V	$C_{19}H_{20}N_6OS$	261-267 °C	0.6

Step 5:

Sr. No.	Compound Code	FT-IR (KBR, cm^{-1})	MASS (m/z %)	1H NMR (400 MHz, DMSO;δ ppm)
1	12a-I	3358 (2° N-H), 3061 (C-H), 1612 (C=N), 1157 (CH_2), 675 (C-S-C)	478 (M+)	4.11-4.16(m, 4H, CH_2-CH_2), 6.91(s, 2H, NH_2), 7.08-7.75(m, 4H, Ph-C_2-C_3-C_5-C_6), 9.7(s, H, NH)
2	12a-II	3290 (2° N-H), 3032 (1° N-H), 2879 (C-H), 1695 (C=N), 675 (C-S-C)	413 (M+2)	5.11-6.53 (m, 4H, Quinazoline Ar-H), 6.90 (d, 2H, NH_2), 7.30-7.98 (m, 2H, Orthophenylene diamine, Ar-H), 8.00-8.02 (m, 4H, Thiadiazole Ar-H), 11.76 (s, 1H, NH),

				11.78 (s, 1H, NH)
3	12a-III	3277 (2° N-H), 3057 (1° N-H), 1546 (C=N), 684 (C-S-C)	400 (M+2)	4.49-5.26 (m, 4H, Quinazoline Ar-H), 6.90-7.98 (m, 4H, Pyrimidine Ar-H), 8.01-8.02 (m, 4H, Thiadiazole Ar-H), 10.93 (s, 1H, NH), 11.06 (s, 1H, NH)
4	12a-IV	3487 (2° N-H), 3182 (C-H), 1583(C=N), 763 (C-F), 688 (C-S-C)	418 (M+2)	6.90-6.99 (m, 4H, Quinazoline Ar-H), 7.04-7.83 (m, 4H, 4-Floroaniline Ar-H), 8.14-8.16 (m, 4H, Thiadiazole Ar-H), 11.05 (s, 1H, NH), 12.23 (s, 1H, NH)
5	12a-V	3252 (OH), 3123 (2° N-H), 3095 (C-H), 1512 (C=N), 1322, 1401 (CH_2 CH_2), 653 (C-S-C)	366 (M+)	3.60-4.05 (t, 4H, CH_2- CH_2), 7.40-7.48 (m, 4H, Quinazoline Ar-H), 7.98-8.11 (m, 4H, Thiadiazole Ar-H), 11.05 (s, 1H, NH), 11.40 (s, 1H, NH), 12.73 (s, 1H, OH)
6	12b-I	3412 (OH), 3290 (2° N-H), 3163 (C-H), 1512 (C=N), 692 (C-S-C)	430(M+)	3.43-3.93 (3, 3H, CH=CH, H), 4.10-4.92 (m, 2H, methyl), 5.11-5.24 (m, 4H, Quinazoline Ar-H), 5.99-7.61(m, 3H, Benzimidazole Ar-H), 7.62-7.89 (m, 4H, Thiadiazole Ar-H), 11.11 (s, 1H, NH), 11.25 (s, 1H, NH), 12.50 (s, 1H, OH)
7	12b-III	3462 (OH), 3355 (2° N-H), 3081 (C-H), 1612 (C=N), 678 (C-S-C)	418 (M+2)	6.90-6.21 (m, 4H, Quinazoline Ar-H), 7.66-7.60 (m, 4H, Pyrimidine Ar-H), 7.93-7.70 (m, 4H, Thiadiazole Ar-H), 11.00 (s, 1H, NH), 11.39 (s, 1H, NH) 12.39 (s, 1H, OH)
8	12b-IV	3456 (OH), 3290 (2° N-H), 3146 (C-H), 1506 (C=N), 754 (C-F), 700 (C-S-C)	430 (M+)	5.45-5.59 (d, 2H, Quinazoline Ar-H), 6.61-6.67 (d, 2H, Quinazoline Ar-H), 7.91-7.60 (m, 4H, 4-Floroaniline Ar-H), 7.61-8.26 (m, 4H, Thiadiazole Ar-H), 10.90 (s, 1H, NH), 11.45 (s, 1H, NH), 12.0 (s, 1H, OH)
9	12c-II	3290 (2° N-H), 3031 (NH_2), 2879 (C-H), 1668 (C=N), 877 (C-F), 684 (C-S-C)	445 (M+)	6.19 (d, 2H, NH_2), 6.87-7.32 (m, 4H, Quinazoline Ar-H), 7.34-7.72 (m, 4H, 4-Orthophenylene, Ar-H), 7.78-8.11 (m, 4H, Thiadiazole Ar-H), 11.19 (s, 1H, NH), 11.40 (s, 1H, NH)
10	12c-IV	3437 (2° N-H), 3184 (C-H), 1591 (C=N), 761 (C-F), 827 (C-Cl), 682 (C-S-C)	450 (M+), 452 (M+2)	5.11-6.90 (m, 4H, Quinazoline Ar-H), 7.30-7.98 (m, 4H, 4-Floroaniline Ar-H), 8.00-8.02 (m, 4H, Thiadiazole Ar-H), 11.17 (s, 1H, NH), 11.32 (s, 1H, NH)
11	12d-II	3454 (2° N-H), 3267 (NH_2), 2992 (C-H), 1658 (C=N), 752 (C-F), 681 (C-S-C)	450 (M+)	3.35-4.54 (m, 4H, Quinazoline Ar-H), 6.91 (d, 2H, NH_2), 6.87-7.63 (m, 2H, Orthophenylene diamine, Ar-H), 7.70-7.96 (m, 4H, Thiadiazole Ar-H), 10.75 (s, 1H, NH),

				11.00 (s, 1H, NH)
12	12d-IV	3433 (2° N-H), 3190 (C-H), 1583 (C=N), 742 (C-F), 678 (C-S-C)	433 (M+)	4.523-4.54 (d, 2H, Quinazoline Ar-H), 5.00-5.25 (m, 2H, Quinazoline Ar-H), 7.11-7.23 (d, 4H, 4-Floroaniline Ar-H), 8.13-8.68 (m, 4H, Thiadiazole Ar-H), 11.42 (s, 1H, NH), 11.66 (s, 1H, NH)
13	12g-IV	3437 (2° N-H), 3184 (C-H), 1537 (C=N), 833 (C-F), 636 (C-S-C)	495 (M+2)	7.25-7.27 (m, 4H, Quinazoline Ar-H), 7.28-7.35 (m, 4H, 4-Floroaniline Ar-H), 7.36-8.17 (m, 4H, Thiadiazole Ar-H), 11.11 (s, 1H, NH), 11.51 (s, 1H, NH)
14	12g-V	3438 (OH), 3331 (2° N-H), 3190 (C-H), 1575 (C=N), 788 (C-F), 681 (C-S-C)	445 (M+), 447 (M+2)	3.35-4.33 (t, 4H, CH_2-CH_2), 7.25-7.32 (m, 4H, Quinazoline Ar-H), 7.34-8.17 (m, 4H, Thiadiazole Ar-H), 11.25 (s, 1H, NH), 11.35 (s, 1H, NH), 12.51 (s, 1H, OH)
15	12e-IV	3402 (2° N-H), 2987 (C-H), 1591 (C=N), 1419 (CH_3), 765 (C-F), 680 (C-S-C)	428 (M+)	3.34 (m, 3H, methyl), 6.64-6.70 (m, 4H, Quinazoline Ar-H), 6.91-7.44 (m, 4H, 4-Floroaniline Ar-H), 7.57-7.84 (m, 4H, Thiadiazole Ar-H), 11.36 (s, 1H, NH), 11.47 (s, 1H, NH)
16	12e-V	3546 (OH), 3446 (2° N-H), 2914 (C-H), 1540 (C=N), 1464 (CH_3), 680 (C-S-C)	428 (M+)	3.60-4.05 (t, 4H, CH_2-CH_2), 7.46-7.52 (m, 4H, Quinazoline, Ar-H), 7.71-7.94 (m, 4H, Thiadiazole Ar-H), 11.33 (s, 1H, NH), 11.60 (s, 1H, NH), 12.71 (s, 1H, OH)

7.6 Biological Activity

7.6.1 Results of In-Vitro Anticancer Screening

Anticancer Activity:

Among the synthesized compounds, compound **12(a-II), 12(a-III), 12(a-IV), 12(b-I), 12(b-III), 12(b-IV), 12(c-II), 12(d-IV), 12(f-IV)** and **12(e-IV)** were tested for in-vitro 96 well MTT assay on A549 cell line (NSCLC) with Cisplatin as positive control at Gujarat University, Ahmedabad. Result of the compound has been obtained. Compound have shown good anticancer activity.

Table 6. Antiproliferative activities of Synthesized Compound

Compound	Code	A-549		
		Conc. (µM)	% Survival	IC50 (µM)
1	12(d-IV)	1000	19.9086758	20.61
		100	31.87214612	
		10	70.68493151	
		1	85.47945205	
		0.1	95.89041096	

		0.01	104.3835616	
2	**12 (f-IV)**	1000	20.3652968	**22.01**
		100	30.1369863	
		10	70.86757991	
		1	82.00913242	
		0.1	94.24657534	
		0.01	95.89041096	
3	**12(b-III)**	1000	21.73515982	74.09
		100	39.36073059	
		10	63.92694064	
		1	81.00456621	
		0.1	89.13242009	
		0.01	102.4657534	
4	**12(a-IV)**	1000	20.3652968	68.02
		100	37.44292237	
		10	69.5890411	
		1	76.52968037	
		0.1	88.94977169	
		0.01	95.70776256	
5	**12(b-IV)**	1000	22.00913242	**12.2**
		100	31.41552511	
		10	62.46575342	
		1	91.05022831	
		0.1	93.51598174	
		0.01	101.2785388	
6	**12(b-III)**	1000	26.48401826	74.88
		100	52.69406393	
		10	86.02739726	
		1	94.61187215	
		0.1	95.70776256	
		0.01	104.0182648	
7	**12(c-II)**	1000	21.55251142	**16.35**
		100	33.60730594	
		10	67.03196347	
		1	79.45205479	
		0.1	97.53424658	
		0.01	107.2146119	
8	**12(b-I)**	1000	18.08219178	**20.76**
		100	29.9543379	
		10	73.88127854	
		1	91.96347032	
		0.1	100.8219178	
		0.01	104.56621	

9	**12(a-III)**	1000	21.73515982	208.06
		100	52.42009132	
		10	64.65753425	
		1	77.26027397	
		0.1	91.87214612	
		0.01	105.2054795	
10	**12(A-II)**	1000	28.49315068	**32.04**
		100	38.90410959	
		10	73.05936073	
		1	76.89497717	
		0.1	88.21917808	
		0.01	95.15981735	
Cisplatin		1000	27.91000011	**33.81**
		100	38.90410959	
		10	73.05936073	
		1	76.89497717	
		0.1	88.21917808	
		0.01	95.15981735	

8. ACHIEVEMENTS WITH RESPECT TO OBJECTIVES

The mentioned objectives in the beginning, which were to find novelty, insilico studies, establish synthetic route, characterize and evaluate anticancer activity of the proposed Quinazoline based-1,3,4- thiadiazole-2yl derivatives and its analogues were carried out. After going through the methodology and results, it is clear that all the objectives were met satisfactorily. Further ADMET studies and preliminary in-vitro MTT assay on NSCLC (A549) cell lines was also carried out for the synthesized new compounds.

9. CONCLUSION

- We have synthesized a series of 6 derivatives of 1,3,4-Thiadiazole **(3a-f)**. Synthesis was carried according to reaction shown in reaction Schemes. 1,3,4-Thiadiazole was prepared using various aromatic carboxylic acid and thiosemicarbazide as starting material. It was confirmed by IR spectra, which showed the presence of amino group stretching at 3281 (-NH_2) and 1626 (C=N) stretching $cm^{-1.}$
- The various 1,3,4-thiadiazole with 2,4-dichloroquinazoline derivatives **(6a-f)** were prepared by condensing the 1,3,4-thiadiazole **(3a-f)** and 2,4-dichloro quinazoline. 1,3,4-thiadiazole with 2,4-dichloroquinazoline derivatives were confirmed by the characteristic IR absorption peak at 815-550 (C-Cl) group, 3281 (-NH_2), 3300 (-NH) cm^{-1}.

- Finally synthesized the proposed compounds having Quinazoline moiety is connected by 1,3,4-thiadiazole moiety at R_1, 2-amino benzimidazole, 2-amino pyrimidine and, different aniline derivatives such as (para fluoro aniline, orthophenylene diamine and ethanolamine) at R_2 **(12a(I-V) to 12f(I-V)).** The reaction was monitored by Thin-layer chromatography using suitable mobile phase such as n-hexane and ethyl acetate (7:3). The R_f values were compared and found that they were different from each other. The melting point of the derivatives was determined.
- The synthesized compound **12(a-II), 12(a-III), 12(a-IV), 12(b-I), 12(b-III), 12(b-IV), 12(c-II), 12(d-IV), 12(f-IV)** and **12(e-IV)** were evaluated for their *in-vitro* anticancer activity at **Gujarat University, Ahmedabad** by **MTT** assay. And showed encouraging anticancer activity.
- Compound **12(b-IV), 12(c-II), 12(b-I), 12(d-IV), 12(f-IV)** and **12(a-II)** showed maximum inhibition IC_{50} value respectively (12.2 µM, 16.35 µM, 20.61 µM, 20.76 µM, 22.01 µM, and 32.04 µM) against **Non-small cell Lung Cancer (A549)** cell line with respect to **cisplatin** as a standard drug.

10. COPIES OF PAPERS PUBLISHED AND A LIST OF ALL PUBLICATIONS ARISING FROM THE THESIS

1. **Published:** Sidat PS, Jaber TMK, Vekariya SR, Mogal AM, Patel AM, Noolvi M. Anticancer Biological Profile of Some Heterocylic Moieties-Thiadiazole, Benzimidazole, Quinazoline, and Pyrimidine. Pharmacophore. 2022;13(4):59-71. https://doi.org/10.51847/rT6VE6gESu
2. **Published:** Parin Sidat, Malleshappa Noolvi, Rahul Patil, Sanket Rathod. ULK1/2 Inhibitor: Essential Component of Autophagic Cell Death Machinery.J. Pharm. Res. 2022;21(3):55–69. https://doi.org/10.18579/jopcr/v21i3.4
3. N Noolvi Malleshappa*, **Salim Sidat Parin**, *et. al;* Exploration of Virtually Designed and Developed Thiadiazole Derivatives as ULK1/2 Inhibitors: In silico Approach, Letters in Drug Design & Discovery 2023; 20(x) (Scopus) http://dx.doi.org/10.2174/1570180820666230825103609
4. **Sidat P**, *et.al;* "Synthesis, DFT Studies, and Biological Evaluation of new quinazoline-1,3,4-thiadiazole Derivatives as anti-proliferative agents", has been accepted for publication in Chemistry Africa. (Scopus) https://www2.cloud.editorialmanager.com/chaf/default2.aspx

11. References

1. Siegel RL, Miller KD, Jemal A. Cancer statistics, 2020. CA Cancer J Clin. 2020;70(1):7–30.
2. Koo MM, Swann R, McPhail S, Abel GA, Elliss-Brookes L, Rubin GP, et al. Presenting symptoms of cancer and stage at diagnosis: evidence from a cross-sectional, population-based study. Lancet Oncol [Internet]. 2020;21(1):73–9. Available from: http://dx.doi.org/10.1016/S1470-2045(19)30595-9
3. Siddiqui MJA, Jafri A, Khan RR. JIPBS Review article Role of environment in development of cancer. 2017;(October 2016).
4. Key TJ, Bradbury KE, Perez-Cornago A, Sinha R, Tsilidis KK, Tsugane S. Diet, nutrition, and cancer risk: What do we know and what is the way forward? BMJ [Internet]. 2020;368(March):1–9. Available from: http://dx.doi.org/doi:10.1136/bmj.m511.
5. Key TJA. Hormones and cancer in humans. Mutat Res - Fundam Mol Mech Mutagen. 1995;333(1–2):59–67.
6. Sauter ER. Cancer prevention and treatment using combination therapy with natural compounds. Expert Rev Clin Pharmacol [Internet]. 2020;13(3):265–85. Available from: https://doi.org/10.1080/17512433.2020.1738218.
7. Jabo B, Lin AC, Aljehani MA, Ji L, Morgan JW, Selleck MJ, et al. Impact of Breast Reconstruction on Time to Definitive Surgical Treatment, Adjuvant Therapy, and Breast Cancer Outcomes. Ann Surg Oncol [Internet]. 2018;25(10):3096–105. Available from: https://doi.org/10.1245/s10434-018-6663-7.
8. Dickens E, Ahmed S. Principles of cancer treatment by chemotherapy. Surg (United Kingdom) [Internet]. 2018;36(3):134–8. Available from: https://doi.org/10.1016/j.mpsur.2017.12.002.
9. Hayat MA. Overview of autophagy. Vol. 12, Autophagy: Cancer, Other Pathologies, Inflammation, Immunity, Infection, and Aging Volume 12. 2017. 1–122 p.
10. Piacentini M, Kroemer G. Dying to survive - Apoptosis, necroptosis, autophagy as the supreme experiments of nature. Int J Dev Biol. 2015;59(1–3):5–9.
11. Schneidman-Duhovny D, Dror O, Inbar Y, Nussinov R, Wolfson HJ. PharmaGist: a webserver for ligand-based pharmacophore detection. *Nucleic Acids Res*. 2008;36(Web Server issue). Doi: 10.1093/nar/gkn187
12. Schneidman-Duhovny D, Dror O, Inbar Y, Nussinov R, Wolfson HJ. Deterministic pharmacophore detection via multiple flexible alignment of drug-like molecules. In: *Journal*

of Computational Biology. Vol 15. ; 2008:737-754. Doi: 10.1089/cmb.2007.0130.

13. WebGro | UAMS. https://simlab.uams.edu/. Accessed May 22, 2022.

14. Joshi M, Singh S, Patel S, Shah D, Krishnakumar A. Identification of small molecule activators for ErbB 4 receptor to enhance oligodendrocyte regeneration by *in silico* approach. *Computational Toxicology*. 2018;8:13-20. Doi: 10.1016/j.comtox.2018.08.004.

15. Hollingsworth SA, Dror RO. Molecular Dynamics Simulation for All. *Neuron*. 2018;99(6):1129-1143. Doi: 10.1016/j.neuron.2018.08.011.

16. Ratra S, Naseer A, Kumar U. Design, Docking, ADMET and PASS Prediction Studies of Novel Chromen-4-one Derivatives for Prospective Anti-Cancer Agent. *Journal of Pharmaceutical Research International*. October 2021:10-22. Doi: 10.9734/jpri/2021/v33i46b32909

17. Molinspiration Cheminformatics. https://www.molinspiration.com/. Accessed May 2, 2022

18. Wang Z, Deng X, Xiong S, Xiong R, Liu J, Zou L, et al. Design, synthesis and biological evaluation of chrysin benzimidazole derivatives as potential anticancer agents. Nat Prod Res [Internet]. 2018;32(24):2900–9. Available from: http://doi.org/10.1080/14786419.2017.1389940.

19. Huang ST, Hsei IJ, Chen C. Synthesis and anticancer evaluation of bis(benzimidazoles), bis(benzoxazoles), and benzothiazoles. Bioorganic Med Chem. 2006;14(17):6106–19.

20. Synthesis and evaluation of new benzimidazole derivatives with hydrazone moiety as anticancer agents Hidrazon yapısı içeren yeni benzimidazol türevlerinin sentezi ve antikanser ajan olarak değerlendirilmesi. 2018;3–10.

1. **Research article -1**

Research Article

Exploration of Virtually Designed and Developed Thiadiazole Derivatives as ULK1/2 Inhibitors: In silico Approach

Author(s): Malleshappa N Noolvi*, Parin Salim Sidat, Sanket Rathod, Rahul Patil, Prafulla Choudhari3, Raj Wagh and Vishal Beldar

(E-pub Abstract Ahead of Print)

DOI: 10.2174/1570180820666230825103609

Price: $95

2. **Research article -2**

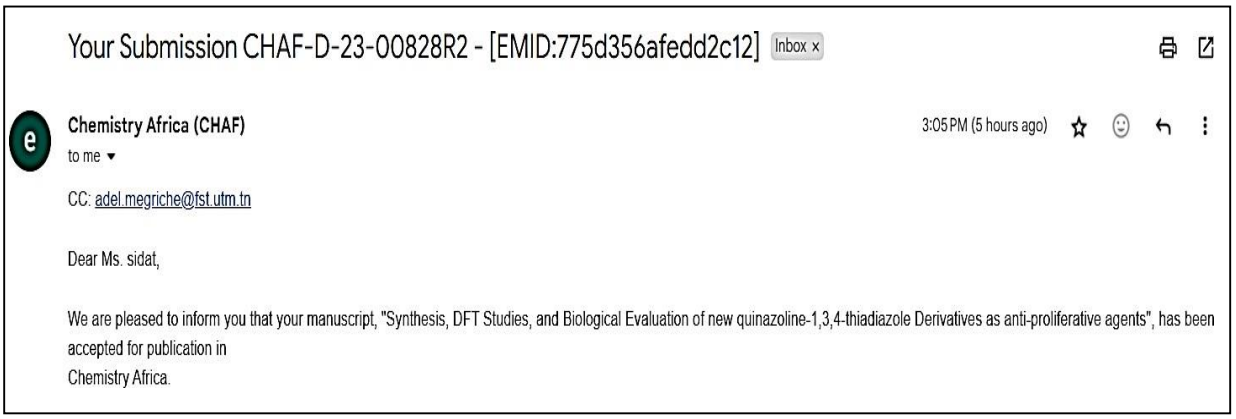

Your Submission CHAF-D-23-00828R2 - [EMID:775d356afedd2c12] Inbox x

Chemistry Africa (CHAF)
to me

3:05 PM (5 hours ago)

CC: adel.megriche@fst.utm.tn

Dear Ms. sidat,

We are pleased to inform you that your manuscript, "Synthesis, DFT Studies, and Biological Evaluation of new quinazoline-1,3,4-thiadiazole Derivatives as anti-proliferative agents", has been accepted for publication in
Chemistry Africa.

Pharmacophore, 13(4) 2022, Pages: 59-71

Pharmacophore

ISSN-2229-5402

Journal home page: http://www.pharmacophorejournal.com

ANTICANCER BIOLOGICAL PROFILE OF SOME HETEROCYLIC MOIETIES-THIADIAZOLE, BENZIMIDAZOLE, QUINAZOLINE, AND PYRIMIDINE

Parin Salim Sidat[1,2]*, Tasneem Mohamadbin Kasim Jaber[2], Shwetang Ramesh Vekariya[2], Azmin Mahervan Mogal[2], Aarifa Mustak Patel[2], Malleshappa Noolvi[2]

1. *Pharmacy Branch, Gujarat Technological University, Ahmedabad, Gujarat, India.*
2. *Department of Pharmaceutical Chemistry, Shree Dhanvantary Pharmacy College, Kim-394110, Gujarat, India.*

ARTICLE INFO

Received:
10 Apr 2022
Received in revised form:

ABSTRACT

Several five and six-membered aromatic systems with three heteroatoms such as S, O, and N have been intensively researched due to their intriguing pharmacological properties. Heterocyclic compounds are chemicals that allow life to exist. Aside from that, all heteroatoms in the ring interact better with amino acids, and these interactions aid in reducing transactivation, and enhancing

J. Pharm. Res. 2022;21(3):55–69

Print ISSN: 0973-7200
Online ISSN: 2454-8405

Journal of Pharmaceutical Research

Review Article

ULK1/2 Inhibitor: Essential Component of Autophagic Cell Death Machinery

Parin Sidat[1,2,*], Malleshappa Noolvi[2], Rahul Patil[3], Sanket Rathod[4]

[1]*Ph. D. Scholar, Pharmacy Branch, Gujarat Technological University, Ahmedabad, Gujarat, India*
[2]*Department of Pharmaceutical Chemistry, Shree Dhanvantary Pharmacy College, Kim, 394110, Gujarat, India*
[3]*Department of Pharmaceutics, Shree Dhanvantary Pharmacy College, Kim, 394110, Gujarat, India*
[4]*Department of Pharmaceutical Chemistry, Bharati Vidyapeeth College of Pharmacy, Kolhapur, 416 013, India*

ARTICLE INFO

Article history:
Received 18.08.2022
Revised 20.09.2022
Accepted 29.09.2022
Published 08.12.2022

ABSTRACT

The effectiveness of selective drug therapy for cancer patients has gained much attention from academics and society. However, the rapid development of the drug resistance gained is becoming a significant challenge. As an essential catabolic and homeostatic process, autophagy plays a vigorous role in the degradation or recycling of proteins and cellular components, by which eukaryotic cells recycle or degrade their internal constituents through the machinery of membrane trafficking. Therefore, under traumatic